JOURNAL OF GUIDANCE, CONTROL, AND DYNAMICS
Vol. 26, No. 5, September–October 2003

Satellite Collision Probability for Nonlinear Relative Motion

Russell P. Patera*
The Aerospace Corporation, Los Angeles, California 90009-2957

A method for calculating the collision probability between two space vehicles when the relative motion is nonlinear is developed using contour integration methodology. The method involves transforming the problem to a scaled frame in which the error covariance matrix is symmetric in three dimensions. This enables the calculation of probability increments as a function of time throughout the encounter. Thus, changes in space vehicle position, velocity, and error covariance matrices throughout the encounter can be included in the formulation. This method is applicable to low-velocity space vehicle encounters that involve nonlinear relative motion. A software tool was created and exercised with both hypothetical and actual satellite data to demonstrate the method. Results differed from those of a Monte Carlo simulation by only 2%. Only 6% error resulted for a stress case in which the exact solution was known.

Nomenclature

C_i	=	covariance matrices in local frame
C_T	=	combined covariance in inertial frame
C_{Td}	=	combined covariance in diagonal frame
$d\theta$	=	contour integration angle
f_i	=	point in hard-body volume
P_i	=	local-to-inertial transformation
PR_I	=	incremental collision probability
$PR_R(t)$	=	collision probability rate
PR_T	=	cumulative collision probability
Q	=	inertial-to-diagonal transformation matrix
r	=	radial cylindrical coordinate
S	=	diagonal-to-scaled frame transformation matrix
U	=	transformation matrix for local to encounter frame
$\boldsymbol{V}$	=	relative velocity vector
$\boldsymbol{V}_S$	=	relative velocity in the scaled frame
$\boldsymbol{V}_Z$	=	velocity in the z direction
W	=	transformation matrix from scaled-to-encounter frame
$\boldsymbol{X}$	=	relative position
X_i	=	point on hard-body area perimeter
$\boldsymbol{X}_S$	=	relative position in scaled frame
z	=	axial cylindrical coordinate
$\sigma(i)$	=	standard deviations of error covariance for each axis in diagonal frame

Introduction

SATELLITE collision probability depends on the trajectory, hard-body size, and error covariance matrix of the respective satellites. In computing collision probability vehicle state vectors are used to propagate the vehicles to points near their closest approach distance. Three-dimensional position error covariance matrices define the position uncertainty for each vehicle. If the uncertainties are uncorrelated, as is usually the case, the error covariances are added to obtain the relative position error.[1] The collision encounter region can be defined by the position-error probability density associated with the combined position-error covariance matrix. Surfaces of constant probability density are ellipsoidal in shape. Because the surface associated with three standard deviations enclosed nearly all of the probability density, the encounter region can be defined by the three-sigma position-error ellipsoid illustrated in the upper portion of Fig. 1.

The collision probability is obtained by integrating the relative position probability density over the volume swept out by the combined hard body during the encounter. Near the encounter region orbital perturbations produce negligible relative acceleration. Thus, the relative velocity is essentially constant throughout the encounter as illustrated in the upper portion of Fig. 1. In addition, because we account for three standard deviations in the encounter region the integral can be extended from minus infinity to plus infinity without introducing error greater than 0.3%. Current collision probability methods increase the limits of integration in this manner to simplify the problem, because the integral of the position error probability density along the velocity vector is unity.

Once the integration along the velocity direction is performed, the problem reduces to evaluating the integral of the relative-error probability density over the projection of the combined hard-body volume to a plane perpendicular to the relative velocity vector referred to as the encounter plane.[2–4] Because the encounter plane can be defined by position and velocity at any point on the linear relative trajectory, one need not propagate the vehicles to the point of closest approach. One need only propagate the vehicles to the region of linearity as illustrated by point A in the upper portion of Fig. 1. The region of linearity depends on the relative encounter velocity but must be larger than the three-sigma position error ellipsoid discussed earlier.

A coordinate rotation in the encounter plane serves to diagonalize the two-dimensional error covariance matrix. A scale change symmetrizes the probability density. The probability density is then integrated in the radial direction, which reduces the problem to that of evaluating a one-dimensional contour integral about the hard-body area in the encounter plane. The contour integration method has already been applied to calculating the collision probability for asymmetric space vehicles[5] and space tethers.[6]

The linear relative motion region might be smaller than the encounter region for very low relative velocity, as illustrated in the lower portion of Fig. 1. Even if one propagates to the point of closest approach and applies current methods, an incorrect collision probability will be obtained.

The correct value of collision probability for low relative velocity requires a numerical integration of the probability density through the volume swept out by the combined hard body of the space vehicles. This integration is complicated by the changing orientation of the hard body and combined position-error ellipsoid throughout the encounter. In addition, integration limits on this volume integral complicate the problem.

The method presented in this work provides exact solutions for cases involving linear relative motion. For cases involving nonlinear

Presented as Paper 2002-4632 at the AIAA/ASS Astrodynamics Specialist Conference, Monterey, CA, 5–8 August 2002; received 7 November 2002; revision received 21 April 2003; accepted for publication 15 May 2003.

*Senior Engineering Specialist, P.O. Box 92957.

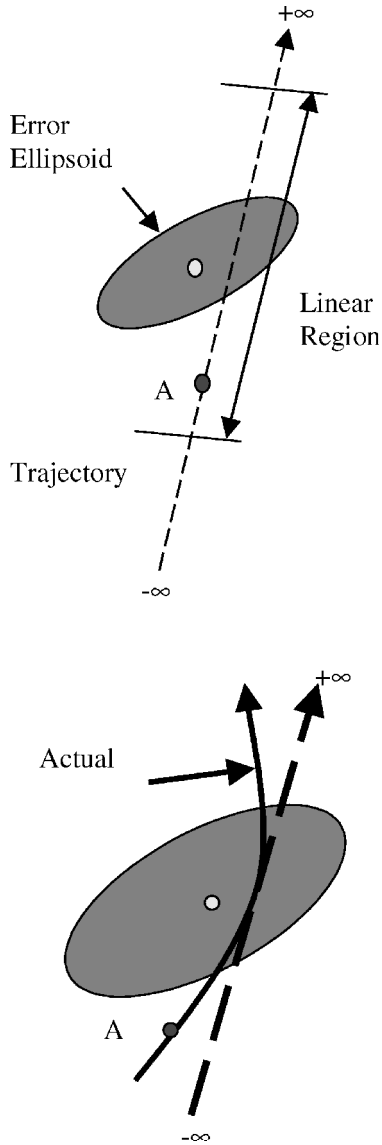

Fig. 1 Linear and nonlinear encounter trajectories.

relative motion, this method provides solutions differing by only a few percent from exact solutions. This accuracy is sufficient to quantify the collision risk. The problem is addressed by transforming to a scaled coordinate frame in which the combined-error covariance matrix is symmetric in three dimensions. In the scaled frame the dimension parallel to the relative velocity vector decouples from the other two dimensions, thereby permitting inclusion of time dependence in collision probability parameters. Thus, the method is valid for cases where the relative velocity varies throughout the encounter region.

Nonlinear Collision Probability Prediction

The general formulation for nonlinear relative motion requires the ability to compute the instantaneous rate of collision probability for a series of time points spanning the encounter. The position, velocity, and position-error covariance matrix for each space vehicle are propagated to each time point. The instantaneous rate of collision probability for each time point is calculated. The total probability of collision over a specified time is obtained by integrating the collision rate over the appropriate time interval.

The instantaneous collision probability is obtained by transforming the problem into a scaled space, where the relative position-error probability density is symmetric in three dimensions. One must transform the relative position-error covariance matrix, the associated position and velocity vectors, as well as the combined hard-body volume to the scaled space.

The local coordinate frame for each space vehicle is defined with the x axis directed in the forward horizontal direction, the z axis directed toward nadir, and the y axis completing the right-handed system. The transformations from local to inertial frame are given by P_1 and P_2, respectively. The respective covariance matrices, which are defined in the local frame, are transformed to the inertial frame in the usual manner:

$$C_{1I} = P_1 C_1 P_1^{-1} \tag{1}$$

$$C_{2I} = P_2 C_2 P_2^{-1} \tag{2}$$

Because the position errors are assumed to be uncorrelated, the error covariance matrices are added to obtain the relative position error covariance matrix in inertial space:

$$C_T = C_{1I} + C_{2I} \tag{3}$$

The transformation from the inertial frame to the frame in which C_T is diagonal is given by Q:

$$C_{\mathrm{Td}} = QC_T Q^{-1} = \begin{bmatrix} \sigma(1)^2 & 0 & 0 \\ 0 & \sigma(2)^2 & 0 \\ 0 & 0 & \sigma(3)^2 \end{bmatrix} \tag{4}$$

Another transformation is made by scaling any two axes to match the third, thus symmetrizing the probability density. This scaling transformation makes the position-error probability density symmetric in three dimensions:

$$S = \begin{bmatrix} 1 & 0 & 0 \\ 0 & \dfrac{\sigma(1)}{\sigma(2)} & 0 \\ 0 & 0 & \dfrac{\sigma(1)}{\sigma(3)} \end{bmatrix} \tag{5}$$

The relative-error covariance matrix in the scaled frame is found in the usual manner:

$$C_{\mathrm{TS}} = SC_{\mathrm{Td}}S^{-1} = \begin{bmatrix} \sigma(1)^2 & 0 & 0 \\ 0 & \sigma(1)^2 & 0 \\ 0 & 0 & \sigma(1)^2 \end{bmatrix} \tag{6}$$

The relative position and velocity in the inertial frame are given by

$$\boldsymbol{X} = \boldsymbol{r}_2 - \boldsymbol{r}_1 \tag{7}$$

$$\boldsymbol{V} = \boldsymbol{u}_2 - \boldsymbol{u}_1 \tag{8}$$

The relative position and velocity vectors are transformed from the inertial frame to the scaled frame:

$$\boldsymbol{X}_S = SQ\boldsymbol{X} \tag{9}$$

$$\boldsymbol{V}_S = SQ\boldsymbol{V} \tag{10}$$

Each time increment has an associated encounter frame. The relative position and velocity vectors in the scaled frame are used to define the transformation to the encounter frame, which has its z axis parallel to the relative velocity vector. The x axis of the encounter frame is orthogonal to the z axis and is directed toward vehicle number one located at the origin. Because the transformation from the scaled frame to the encounter frame W is an orthogonal transformation and the relative-error covariance is symmetric, the error covariance remains unchanged in the encounter frame:

$$C_{\mathrm{Te}} = WC_{\mathrm{TS}}W^{-1} = C_{\mathrm{TS}} \tag{11}$$

The hard-body volume, which is assumed centered about space vehicle number two, is transformed to the inertial frame and then to the scaled frame. The hard-body volume is then projected to the encounter plane, which is the x-y plane in the encounter frame.

Any point f_i within the hard-body volume can be transformed to the encounter frame by the transformation U, which is given by

$$f_{\mathrm{ie}} = WSQP_2 f_i = Uf_i \tag{12}$$

Because the probability density is symmetric, the probability density along each axis is decoupled from the other axes in the encounter frame. The cumulative collision probability is given by

$$PR_T = \frac{1}{(2\pi)^{3/2}\sigma(1)^3} \iiint_{\text{vol}} \exp\left[\frac{-(x^2+y^2+z^2)}{2\sigma(1)^2}\right] \mathrm{d}x\,\mathrm{d}y\,\mathrm{d}z \tag{13}$$

where the limits of integration are defined by the volume swept out by the hard body in the encounter frame. Because z is in the direction of relative velocity, it is convenient to transform to cylindrical coordinates with the z axis aligned with the cylinder axis. The cumulative collision probability becomes

$$PR_T = \frac{1}{(2\pi)^{3/2}\sigma(1)^3} \iiint_{\text{vol}} \exp\left[\frac{-z^2}{2\sigma(1)^2}\right] \times \exp\left[\frac{-r^2}{2\sigma(1)^2}\right] r\,\mathrm{d}r\,\mathrm{d}\theta\,\mathrm{d}z \tag{14}$$

The integration along the z axis is made in incremental steps assuming that probability density, hard-body area, and relative velocity are constant over each time step. For each increment the r integration can be performed immediately, yielding

$$PR_I = \left\{\frac{1}{\sqrt{2\pi}\sigma(1)} \int_{-\Delta}^{\Delta} \exp\left[\frac{-z^2}{2\sigma(1)^2}\right] \mathrm{d}z\right\}\left(\frac{1}{2\pi}\right) \times \oint_{\text{perimeter}} \left\{1 - \exp\left[\frac{-r^2}{2\sigma(1)^2}\right]\right\} \mathrm{d}\theta \tag{15}$$

where the closed-path contour is about the perimeter of the hard-body area in the encounter plane. Thus, one has a finite number of cylindrical volumes, each with an associated collision probability. If the relative velocity and relative-error covariance are constant, the cylindrical increments can be combined to form a single cylinder extending from minus infinity to plus infinity. The integration of this infinite cylinder in Eq. (15) (bracketed term) is equal to one, and the cumulative collision probability is given by

$$PR_C = \left(\frac{1}{2\pi}\right) \oint_{\text{perimeter}} \left\{1 - \exp\left[\frac{-r^2}{2\sigma(1)^2}\right]\right\} \mathrm{d}\theta \tag{16}$$

Equation (16) is equivalent the method developed in Ref. 5. The expression in the exponential term of Eq. (16) has a simpler form than the equivalent expression in Ref. 5. Equation (16) is used in evaluating collision probability for cases involving linear relative motion.

If the relative velocity or the relative-error covariance changes, one should first obtain the incremental collision probability given in Eq. (15), which can be written as

$$PR_I = \left\{\frac{\Delta z}{\sqrt{2\pi}\sigma(1)} \exp\left[\frac{-z^2}{2\sigma(1)^2}\right]\right\}\left(\frac{1}{2\pi}\right) \times \oint_{\text{perimeter}} \left\{1 - \exp\left[\frac{-r^2}{2\sigma(1)^2}\right]\right\} \mathrm{d}\theta \tag{17}$$

Equation (16) can be used in Eq. (17) to obtain

$$PR_I = \frac{\Delta z}{\sqrt{2\pi}\sigma(1)} \exp\left[\frac{-z^2}{2\sigma(1)^2}\right] PR_C \tag{18}$$

Both Δz and $\sigma(1)$ are permitted to change during the encounter but are considered constant for each individual volume increment. The symmetrization process ensures that $\sigma(2)$ and $\sigma(3)$ change with $\sigma(1)$.

Because the velocity direction changes from cylindrical increment to cylindrical increment, there are overlaps and gaps between adjacent cylinders. Volumes associated with the overlaps and gaps are exactly equal. Thus, if the probability density remains constant over each incremental volume the probabilities associated with overlaps and gaps are equal. In this manner the gaps and overlaps compensate so that no net error is introduced. However, if the probability density changes throughout each incremental volume some error is introduced. This error is small as long as the hard body is significantly smaller than the position-error ellipsoid, which is usually the case. This assertion is supported by a numerical study presented in the Numerical Results section, which found a collision probability error of only 2% for a hard-body radius equal to 30% of the one-sigma position uncertainty.

The collision probability rate can be obtained by dividing Eq. (18) by the time increment associated with Δz:

$$PR_R(t) = \left(\frac{\Delta z}{\sigma(1)\Delta t}\right)\left(\frac{1}{\sqrt{2\pi}}\right) \exp\left[\frac{-z^2}{2\sigma(1)^2}\right] PR_C \tag{19}$$

If the increments are made sufficiently small, $\Delta z/\Delta t$ can be approximated with the velocity along the z axis, V_Z. Thus,

$$PR_R(t) = \left[\frac{V_z}{\sigma(1)}\right]\left(\frac{1}{\sqrt{2\pi}}\right) \exp\left[\frac{-z^2}{2\sigma(1)^2}\right] PR_C \tag{20}$$

The collision probability rate is evaluated for a set of times spanning the encounter. The collision probability rates are integrated over the time of interest to obtain the total collision probability associated with the time interval from t_1 to t_2:

$$PR = \int_{t1}^{t2} PR_R(t)\,\mathrm{d}t \tag{21}$$

The time duration associated with Eq. (20) depends on the dynamics of each particular encounter. The number of steps required is found in the usual manner by simply increasing the number of steps until the resulting probability does not vary appreciably with increasing number of steps. It will be shown that several hundred time steps over the encounter duration provide sufficient accuracy for computing collision probability.

If a trajectory is highly nonlinear, the hard body can sweep through a volume of space at one time and return to sweep through the same space again. Thus, in implementing Eq. (21) one must consider the volume being swept out by the hard body as it moves along its nonlinear trajectory and ensure that the volume is swept out only once. Extreme cases where the relative velocity direction changes enough to cause the same volume to be swept out more than once will be treated in a future work and will not be considered here.

Nevertheless, Eq. (21) works well for most nonlinear space vehicle encounters. Such encounters typically sweep through regions of significant spatial probability density only once and involve combined hard-body sizes that are significantly less than the associated standard deviations of relative position uncertainty. For typical encounters simulated test cases indicate that only a few percent error in computed collision probability result.

Numerical Integration About Contour

The cross-track contour integration over the hard-body region is performed for each incremental time step. The shape of the contour and the value of the integral can change for each increment because of changes in relative velocity, probability density, etc.

The following computation is performed for each time increment. Space vehicle number one is located at the origin of the encounter frame, which is also the center of the relative position-error probability density. The location of space vehicle number two is found by transforming its relative displacement from vehicle one to the encounter plane. The hard-body volume is centered on the space vehicle number two. Points defining the shape of the hard-body volume are transformed to the encounter plane. These points are used in the evaluation of the contour integral, as shown in Fig. 2. The points are enumerated sequentially in a counterclockwise direction about the perimeter.

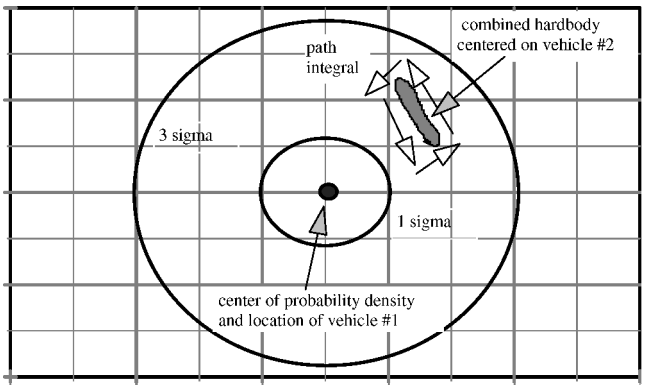

Fig. 2 Contour integration path in symmetrized encounter plane.

The angle between the two adjacent vectors $\boldsymbol{X}_i$ and $\boldsymbol{X}_{i+1}$, is given by $\mathrm{d}\theta_i$. By noting its relationship to the cross product between the two vectors, $\mathrm{d}\theta_i$ can be obtained from

$$|\boldsymbol{X}_i \times \boldsymbol{X}_{i+1}| = |\boldsymbol{X}_i||\boldsymbol{X}_{i+1}| \sin(\mathrm{d}\theta_i) \tag{22}$$

After rearranging Eq. (22), one finds

$$\mathrm{d}\theta_i = \sin^{-1}\left(\frac{|\boldsymbol{X}_i \times \boldsymbol{X}_{i+1}|}{|\boldsymbol{X}_i||\boldsymbol{X}_{i+1}|}\right) \tag{23}$$

If the total number of points used in completing one circuit about the contour is n, then $\boldsymbol{X}_{n+1}$ is $\boldsymbol{X}_1$.

The exponential term in the ith integrand is evaluated as

$$\mathrm{int}_i = \exp\left[\frac{-\left(\boldsymbol{X}_i^2 + \boldsymbol{X}_{i+1}^2\right)}{4\sigma(1)^2}\right] \tag{24}$$

The integral is evaluated by summing values of the integrand times $d\theta_i$ for each pair of points around the contour:

$$\mathrm{sum} = \sum_{i=1}^{i=n} \mathrm{int}_i \, \mathrm{d}\theta_i \tag{25}$$

Once one complete cycle about the ellipse is made, the cumulative probability is given by Eq. (16) as

$$PR_T = \frac{-\mathrm{sum}}{2\pi} \tag{26a}$$

$$PR_T = 1 - \frac{\mathrm{sum}}{2\pi} \tag{26b}$$

where the origin is excluded from the hard-body region in Eq. (26a) and included in the hard-body region in Eq. (26b).

Numerical Results

A simulation was developed to test the accuracy of the methodology. A case involving two objects in low Earth orbit having constant relative velocity throughout the encounter was examined. Relative separation distance, collision probability assuming linear relative motion, and nonlinear collision probability are plotted as functions of time in Fig. 3. Because the relative velocity is constant, the linear assumption is valid and gives the correct collision probability at all times throughout the encounter. The nonlinear collision probability is zero until the relative position enters the region of significant probability density, which is defined by the three-sigma position-error ellipsoid. As the encounter progresses, the collision probability increases until the relative position is again beyond the region of significant probability. At the end of the encounter, the nonlinear collision probability equals the linear collision probability, as it must. Notice that the region of highest probability density is not at the point of closest approach between the two objects. This result, although counterintuitive, is correct and is caused by the orientation and eccentricity of the combined position-error ellipsoid. In this case

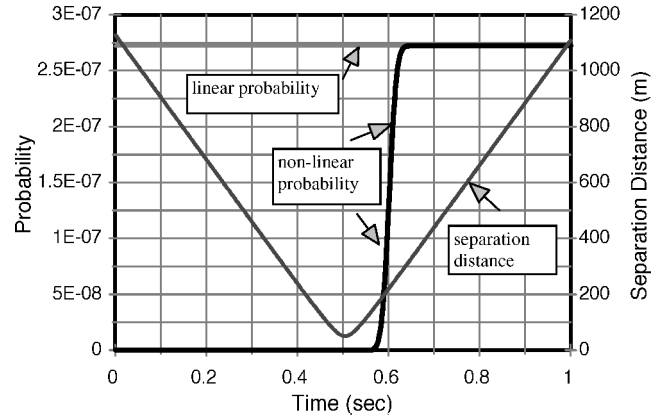

Fig. 3 Comparison of linear and nonlinear collision probability for a linear relative motion encounter.

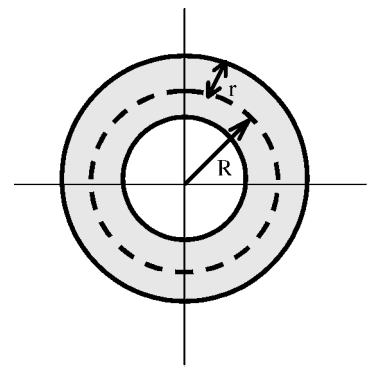

Fig. 4 Circular relative motion trajectory test case.

the largest ellipsoid axis is oriented in roughly the same direction as but not exactly parallel to the relative trajectory. This situation results in the trajectory penetrating the three-sigma ellipsoid at a point past the closest approach point.

A case with continuously varying velocity was chosen to stress the nonlinear collision probability algorithm. A circular trajectory was chosen because the exact collision probability could be obtained easily. A spherical hard-body radius and a spherically symmetric position error distribution were assumed to simplify the computation. The spherical hard body carves out a toroidal volume as the vehicle orbits the origin in the relative motion frame. The standard deviation of the relative position uncertainty was set equal to the radius of the orbit. The collision probability was found for one orbit about the torus for various sizes of the spherical hard body. Figure 4 illustrates the parameters for the toroidal volume. The exact collision probability is given by

$$p = \frac{2}{\sigma}\sqrt{\frac{2}{\pi}} \exp\left[\frac{-(R^2 + r^2)}{2\sigma^2}\right] \int_0^r \sinh\left(\frac{R\sqrt{r^2 - x^2}}{\sigma^2}\right) \mathrm{d}x \tag{27}$$

where R is the radius of the torus and r is the radius of its cross sectional as illustrated in Fig. 4. A comparison of collision probabilities for various values of r/σ was obtained by varying r with both R and σ equal to one. It was found via simulation that the error depends on the ratio of r/σ and is nearly independent of R. For example, when sigma equals one and r equals 0.3 the error for cases of R equaling one and three are 2.2 and 2.14%, respectively. Thus, the results shown in Fig. 5 are independent of R and indicate that for r/σ equal to one-half of sigma the error is only 6%.

A study was conducted to determine how the number of incremental steps affects the computed value of collision probability. For a value of r/σ of 0.3, the number of steps was varied from 2 to 300. A plot of the resulting collision probability is illustrated in Fig. 6. The correct value of the collision probability is also shown in Fig. 6. As the number of steps increases, the solution does not converge to the exact solution. For $r/\sigma = 0.3$ there is a residual error of about

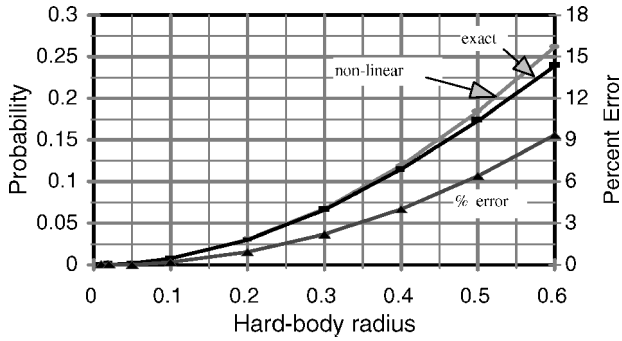

Fig. 5 Error vs hard-body size ratio.

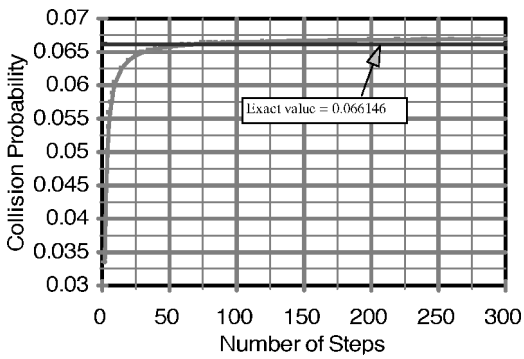

Fig. 6 Convergence of collision probability as a function of the number of trajectory increments.

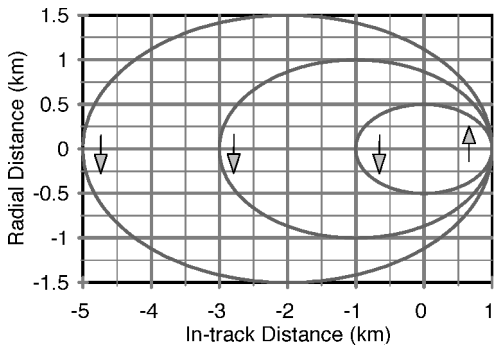

Fig. 7 Relative trajectory for several values of semimajor axis.

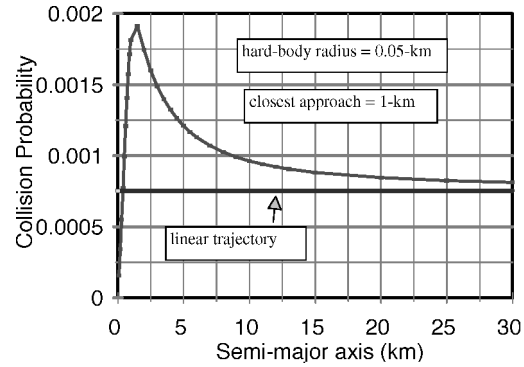

Fig. 8 Collision probability as a function of semimajor axis.

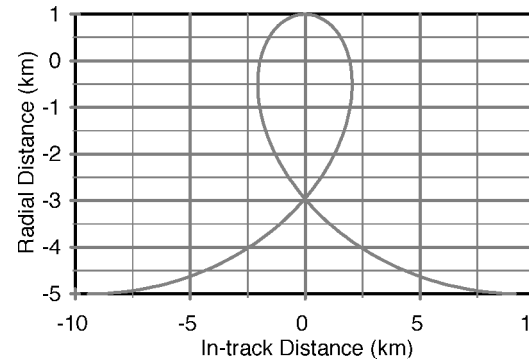

Fig. 9 Relative trajectory for a nonlinear encounter.

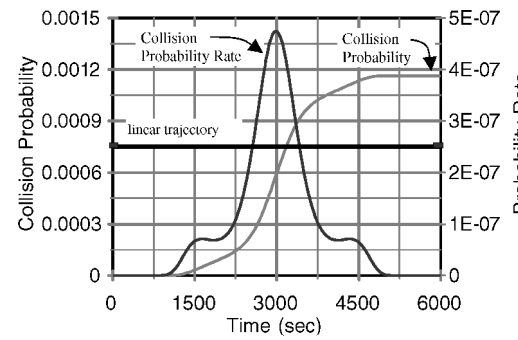

Fig. 10 Collision probability and probability rate for the test case depicted in Fig. 9.

2% as indicated in Fig. 6. As stated earlier, this error arises because of the unmodeled change in velocity direction during each time increment. Figure 6 indicates that the collision probability calculation does not require a large number of steps.

A realistic relative motion trajectory was created by positioning two space vehicles in the same circular orbit. The first vehicle was placed at the origin, whereas the second was displaced 1 km in track. A small radial velocity increment was imparted to the second vehicle so that it would circle the first at the orbital frequency. The velocity was varied to change the size of the semimajor axis of the elliptical trajectory in the relative motion frame. For small radial velocity increments the semiminor axis is one-half of the semimajor axis. Figure 7 illustrates several such elliptical trajectories. The standard deviation of the combined position error was also 1 km. The hard-body radius was 0.05 km. Figure 8 illustrates the change in collision probability vs the size of the semimajor axis. As the semimajor axis increases, the encounter becomes closer to that of a higher velocity linear encounter. The probability of a linear encounter was found from Eq. (16) to be 0.000754 as shown in Fig. 8. The collision probability peaks for semimajor axis of about 1.5 km. For smaller values of semimajor axis, the associated collision probability decreases to less than that of the linear trajectory as indicated in Fig. 8.

Another example of realistic relative orbital motion was examined by placing a vehicle in a 400-n mile circular orbit. A second vehicle was placed 1 km above the first and given a small velocity increment in a direction opposite to the orbital velocity. The resulting relative motion is depicted in Fig. 9. The period and semimajor axis of the second vehicle are less than that of the first. The relative velocity direction changes dramatically throughout the encounter. The standard deviation of the relative position error was 1 km, and the hard-body radius was 0.05 km. Figure 10 illustrates the collision probability as a function of time throughout the encounter. The trajectory begins and ends in regions of very low position probability density to ensure that the entire encounter is captured. The collision probability rate, which peaks at the closest approach distance, is also presented in Fig. 10. As expected, the total collision probability was found to be 0.001164, which is greater than that of the linear trajectory, which was only 0.000754.

The encounter between two geosynchronous satellites with a combined hard-body radius of 100 m was examined and results plotted in Fig. 11. There is a daily cyclic variation in separation distance, which is typical of neighboring geosynchronous satellites. For a period of one day, Keplerian motion is sufficient to model this variation in separation distance for purposes of computing collision

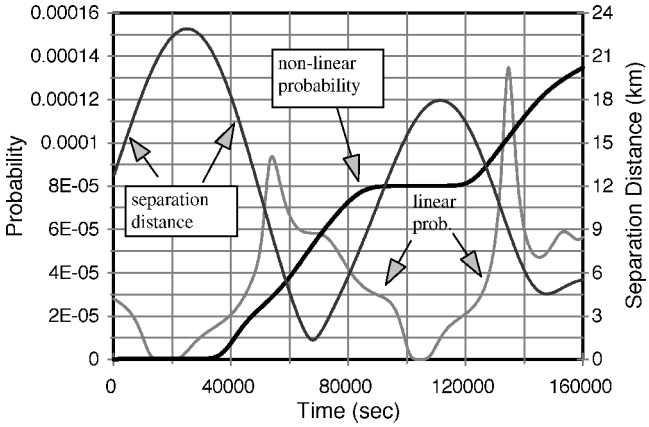

Fig. 11 Comparison of linear and nonlinear collision probability for two adjacent geosynchronous satellites.

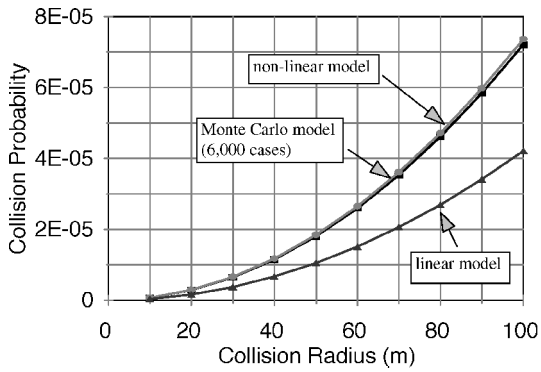

Fig. 12 Comparison of collision probability results for the nonlinear model and a 6000-run Monte Carlo simulation.

probability. The motion is determined by the initial conditions of the two satellites. The linear collision probability obtained using Eq. (16) exhibits large fluctuations as a function of time, indicating that the relative motion is nonlinear. The nonlinear collision probability is well behaved. It increases during each passage through significant probability density near each local minimum separation distance. Thus for collision probability to be meaningful, the associated time duration should be specified. For each particular case Eq. (21) should be used to calculate collision probability producing a plot similar to Fig. 11. The time duration of interest can be determined by examining the resulting figure.

The accuracy of the nonlinear model was determined by comparison with a Monte Carlo simulation for the case depicted in Fig. 11. In the Monte Carlo simulation initial positions were determined by the position-error covariance of each satellite. The closest approach distance for each Monte Carlo case was found via trajectory propagation. A collision resulted if the closest approach distance was less than the combined hard-body distance. In this manner a collision probability vs hard-body size was found. Probabilities for small hard-body sizes were found via extrapolation based on the known linear relationship between collision probability and hard-body cross-sectional area.

The collision probability associated with time duration from 40,000 to 120,000 s in Fig. 11 was computed using the nonlinear model and a Monte Carlo simulation of 6000 runs. The hard-body radius was varied from 0 to 100 m. The nonlinear model produced collision probabilities about 2% greater than those of the Monte Carlo simulation, as illustrated in Fig. 12. However, the nonlinear model required only a very small fraction of the computational effort required of the Monte Carlo simulation. The nonlinear model required only a few seconds, whereas the Monte Carlo simulation required several hours to compute collision probability. Figure 12 also shows results of a linear simulation using vehicle state vectors at 80,000 s.

Conclusions

A general method for calculating the collision probability for nonlinear relative motion was developed. The method is applicable to changing error covariance matrices and changing relative velocity. Both collision probability and collision probability rate were obtained as functions of time. When the relative velocity or error covariance matrix changes over time, then the instantaneous rate of collision probability must be integrated over the time span of interest to obtain the total collision probability. The method is also applicable if the relative velocity and error covariance matrices remain constant.

A computer program was developed to implement the technique. The validity of the method was examined by comparing results to a case with known collision probability. The error introduced by changing relative velocity direction was only 6% when the hard-body size was 50% of the position-error standard deviation.

The method was used on other cases involving realistic orbital motion. The validity of the method was also confirmed using the nonlinear encounter between two geosynchronous satellites and comparing results with those generated via Monte Carlo simulation. The nonlinear model results differed by only 2% from results obtained using 6000 Monte Carlo runs. This illustrates that the method is applicable to nonlinear relative motion trajectories that might be encountered in actual space vehicle operations.

This methodology is particularly useful for geostationary spacecraft, where low-velocity nonlinear encounters are more apt to occur because of the high concentration of spacecraft in similar orbits.

Acknowledgments

The author thanks T. Morehart, R. Gist, S. Alfano, and G. Peterson of The Aerospace Corporation for technical and editorial review of this paper.

References

[1] Chan, K., "Collision Probability Analysis for Earth Orbiting Satellites," *Advances in the Astronautical Sciences*, Vol. 96, July 1997, pp. 1033–1048.

[2] Berend, N., "Estimation of the Probability of Collision Between Two Catalogued Orbiting Objects," *Advances in Space Research*, Vol. 23, No. 1, 1999, pp. 243–247.

[3] LeClair, R. A., "Probability of Collision in the Geostationary Orbit," *Proceedings of the 2000 Space Control Conference*, edited by S. E. Andrews, Lincoln Lab., Massachusetts Inst. of Technology, Lexington, MA, 2000, pp. 85–92.

[4] Alfriend, K. T., Akella, M. R., Lee, D., Frisbee, J., and Foster, J. L., "Probability of Collision Error Analysis," *Space Debris*, Vol. 1, No. 1, 1999, pp. 21–35.

[5] Patera, R. P., "General Method for Calculating Satellite Collision Probability," *Journal of Guidance, Control and Dynamics*, Vol. 24, No. 4, 2001, pp. 716–722.

[6] Patera, R. P., "Method for Calculating Collision Probability Between a Satellite and a Space Tether," *Journal of Guidance, Control, and Dynamics*, Vol. 25, No. 5, 2002, pp. 940–945.